ACCOUNTS
of chemical research

Femtosecond Spectroscopy from the Perspective of a Global Multidimensional Response Function

PATRICK NUERNBERGER, KEVIN F. LEE, AND MANUEL JOFFRE*

Laboratoire d'Optique et Biosciences, Ecole Polytechnique, Centre National de la Recherche Scientifique, 91128 Palaiseau, France, and Institut National de la Santé et de la Recherche Médicale, U696, 91128 Palaiseau, France

Ⓦ This paper contains enhanced objects available on the Internet at http://pubs.acs.org/acr.

CONSPECTUS

At the microscopic level, multidimensional response functions, such as the nonlinear optical susceptibility or the time-ordered response function, are commonly used tools in nonlinear optical spectroscopy for determining the nonlinear polarization resulting from an arbitrary excitation. In this Account, we point out that the approach successfully developed for the nonlinear polarization can also be used in the case of a

directly observable macroscopic quantity. This observable can be, for example, the electric field radiated in a nonlinear mixing experiment, the rate of fluorescence resulting from one- or two-photon absorption, or the rate of a photochemical reaction. For each of these physical processes, perturbation theory can be used to expand the measured quantity in a power series of the exciting field, and an appropriate global response function can be introduced for each order of perturbation. At order n, the multidimensional response function will depend on n variables (either time or frequency) and have the same general properties as the nonlinear susceptibility resulting, for example, from time invariance or causality. The global response function is introduced in this Account in close analogy with the nonlinear susceptibility or the time-ordered microscopic response.
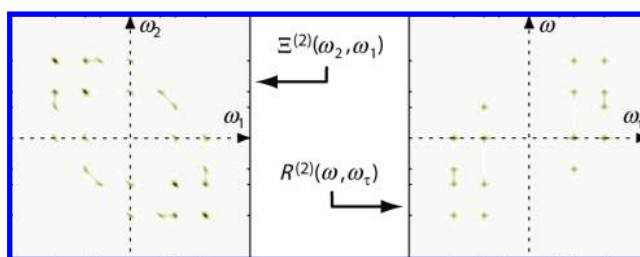
We discuss various applications of the global response function formalism. For example, it can be shown that in the weak field limit, a stationary signal induced in a time-invariant system is independent of the spectral phase of the exciting field. Although this result had been demonstrated previously, the global response function enables its derivation in a more general way because no specific microscopic model is needed.

Multidimensional spectroscopy is obviously ideally suited to measure the global multidimensional response function. It is shown that the second (or third)-order response can be exactly measured with 2D (or 3D) spectroscopy by taking into account the exact shape of the exciting pulses. In the case of a 2D measurement of the third-order response, a particular projection of the complete 3D response function is actually measured. This projection can be related to a mixed time and frequency representation of the response function when the pulses are assumed to be infinitely short.

We thus show that the global response function is a useful tool for deriving general results and that it should help in designing future experimental schemes for femtosecond spectroscopy.

1. Introduction

In nonlinear optics, the properties of matter during light–matter interactions generally have to be described as a multidimensional (tensorial) function. At the microscopic level, the nonlinear polarization induced in a given material is thus entirely determined by the nonlinear response function, which depends on as many variables as the relevant order of perturbation theory. In frequency domain, this multidimensional function can be the nonlinear optical susceptibility,[1] while in time domain, the time-ordered response function is

usually preferred.[2] The purpose of this Account is to show that this very fruitful approach is not limited to the microscopic polarization but can also be applied to a directly observable macroscopic quantity, such as the rate of a chemical reaction or the electric field radiated by a given sample. Although it is not as close to a microscopic description of the system, a global view is more general and can be important for fundamental considerations. The mathematical description is first introduced in a very general way, in analogy with the nonlinear susceptibility or the time-ordered response function. In the second half of the paper, we give examples of the global response function formalism and its applicability to coherent control and multidimensional spectroscopy.

2. Multidimensional Response Function

We consider a signal, $S(t)$, resulting from system excitation by an optical pulse of arbitrary shape. $S(t)$ might be the induced polarization, the field radiated by the sample, the rate of a chemical reaction, or the rate of fluorescence emission. For the sake of simplicity, tensorial aspects will not be considered here and the electric field will be assumed to be a scalar quantity, $E(t)$. However, this could be easily added, following the standard formalism of the nonlinear susceptibility tensor.

We will write

$$E(t) = \frac{1}{2}(\mathcal{E}(t) + \mathcal{E}^*(t)) \tag{1}$$

where $\mathcal{E}(t)$ is the analytic representation, or complex field, associated with the real field $E(t)$. In frequency domain, we have

$$E(\omega) = \frac{1}{2}(\mathcal{E}(\omega) + \mathcal{E}^*(-\omega)) \tag{2}$$

where $\mathcal{E}(\omega)$ is nonzero only for positive frequencies. The field spectrum will be assumed to be centered on the carrier frequency ω_0.

2.1. Symmetrized Response Function. Assuming that the system is excited with a pulse of moderate energy, we will make use of perturbation theory and expand $S(t)$ in a power series

$$S(t) = S^{(1)}(t) + S^{(2)}(t) + S^{(3)}(t) + \dots \tag{3}$$

where $S^{(n)}(t)$ is a multilinear function of the electric field of order n. Throughout this Account, the system will be assumed to be time invariant in the general sense, meaning that a field $E(t - T)$ shifted in time by the constant value T will produce a signal shifted by the same amount, that is, $S(t - T)$. This implies[1] that the multilinear response $S^{(n)}(t)$ takes the form

$$S^{(n)}(t) = \int \Xi^{(n)}(t_n, \dots, t_1)E(t - t_n) \dots E(t - t_1)\, dt_1 \dots dt_n \tag{4}$$

where $\Xi^{(n)}(t_n, \dots, t_1)$ is by definition the appropriate response function at order n. For the sake of simplicity, multiple integrals, all extending from $-\infty$ to $+\infty$ in this Account, are represented by a single integral sign only. Equation 4 will be written hereafter $S^{(n)}(t) \equiv \Xi \otimes [E \dots E]$ (although the integral is not strictly a multidimensional convolution product). Note that causality implies that $\Xi^{(n)}(t_n, \dots, t_1)$ vanishes as soon as one of its arguments is negative. In frequency domain, we obtain

$$S^{(n)}(t) = \int \Xi^{(n)}(\omega_n, \dots, \omega_1)E(\omega_n) \dots E(\omega_1) \times$$
$$\exp(-i(\omega_1 + \dots + \omega_n)t)\, \frac{d\omega_1}{2\pi} \dots \frac{d\omega_n}{2\pi} \tag{5}$$

where $\Xi^{(n)}(\omega_n, \dots, \omega_1)$ is the multidimensional Fourier transform of the real-valued $\Xi^{(n)}(t_n, \dots, t_1)$; hence $\Xi^{(n)}(-\omega_n, \dots, -\omega_1) = \Xi^{(n)}(\omega_n, \dots, \omega_1)^*$. In order to make the response function uniquely defined, it is assumed that $\Xi^{(n)}$ is invariant through the $n!$ possible permutations of its n arguments. In the case where $S^{(n)}(t)$ is the nonlinear polarization $P^{(n)}(t)$, the response function $\Xi^{(n)}(\omega_n, \dots, \omega_1)$ is equivalent to the nonlinear susceptibility, $\chi^{(n)}(\omega_n, \dots, \omega_1)$, as defined in standard nonlinear optics textbooks.[1] If $S^{(n)}(t)$ is the field $E^{(n)}(t)$ radiated by the sample, the response function $\Xi^{(n)}$ is the product of the susceptibility $\chi^{(n)}$ and a term including phase-matching effects.[3,4]

2.2. Time-Ordered Response Function. Another widespread choice of response function, as defined, for example, by Mukamel,[2] explicitly shows the time ordering of the fields. In this case, the nonlinear signal reads

$$S^{(n)}(t) = \int R^{(n)}(t_n, t_{n-1}, \dots, t_1)E(t - t_n) \dots$$
$$E(t - t_n - \dots - t_1)\, dt_1 \dots dt_n \tag{6}$$

Such an integral will be hereafter written $S^{(n)}(t) = R^{(n)} \odot [E \dots E]$. The response function $R^{(n)}(t_n, t_{n-1}, \dots, t_1)$ vanishes as soon as one of its arguments is negative. This ensures that the interactions with the electric field are time ordered, with the field on the right, $E(t - t_n - \dots - t_1)$, corresponding to the first interaction and the field on the left, $E(t - t_n)$, corresponding to the last of the n interactions. Unlike the symmetrized response $\Xi^{(n)}$, the time-ordered response $R^{(n)}$ is not invariant with respect to the permutations of its arguments. As above, we can replace in eq 6 the electric fields with their Fourier transforms:

$$S^{(n)}(t) = \int R^{(n)}(\omega_1 + \dots + \omega_n, \omega_1 + \dots + \omega_{n-1}, \dots, \omega_1) \times$$
$$E(\omega_n) \dots E(\omega_1) \exp(-i(\omega_1 + \dots + \omega_n)t)\, \frac{d\omega_1}{2\pi} \dots \frac{d\omega_n}{2\pi} \tag{7}$$

2.3. Relation between the Symmetrized and Time-Ordered Response Functions. In order to relate the two response functions introduced above, let us introduce the function

$$\xi^{(n)}(t_n, \ldots, t_1) = \Xi^{(n)}(t_n, t_n + t_{n-1}, \ldots, t_n + \ldots + t_1) \quad (8)$$

We then obtain

$$S^{(n)}(t) = \xi^{(n)} \odot [E \ldots E] \quad (9)$$

This expression is very similar to eq 6, with the important difference that, unlike $R^{(n)}$, the function $\xi^{(n)}$ can take nonzero values when its arguments are negative. Another feature specific to $\xi^{(n)}$, which will be quite handy in the following sections, is that $\xi^{(n)} \odot [E_n \ldots E_1]$ is invariant through any permutation of the n fields. The time-ordered and symmetrized response function can be simply related by reordering the $n!$ possible time orderings contributing to eq 4, yielding

$$R^{(n)}(t_n, t_{n-1}, \ldots, t_1) = n! \, \xi^{(n)}(t_n, t_{n-1}, \ldots, t_1) \Theta(t_n) \ldots \Theta(t_1) \quad (10)$$

Conversely, if we compare eq 7 and eq 5, we remark that the function $R^{(n)}(\omega_1 + \ldots + \omega_n, \ldots, \omega_1)$ needs only to be symmetrized in order to comply with the definition of the symmetrized response function. It is therefore straightforward to express one of the two response functions as a function of the other one:

$$\Xi^{(n)}(\omega_n, \ldots, \omega_1) =$$

$$\frac{1}{n!} \sum_{\{n!\}} R^{(n)}(\omega_1 + \ldots + \omega_n, \omega_1 + \ldots + \omega_{n-1}, \ldots, \omega_1) \quad (11)$$

with the sum over the $n!$ permutations of $\{\omega_1, \ldots, \omega_n\}$. Both response functions contain exactly the same amount of information on the system, actually all the information on the generated signal at the corresponding order of perturbation theory. While $R^{(n)}$ contains the frequencies of the system's polarization as its arguments and hence is connected to a certain order of interacting frequencies, $\Xi^{(n)}$ is more general and depends on the frequencies ω_j interacting with the system, covering all possible combinations.

We now apply this general formalism to several aspects of femtosecond spectroscopy.

3. Photodetection

We consider here photodetection in its broader meaning, that is, any mechanism producing a signal sensitive to the optical excitation. This could be photocurrent as in a conventional photodetector but also other physical mechanisms such as flu-

orescence yield or a photochemical reaction (e.g., in the eye). Furthermore, considering the femtosecond time scale of the excitation process, it will be considered that the only relevant quantity is the final result, after the pulse excitation. To apply the formalism of the preceding section, we will assume that $S(t)$ is the instantaneous rate of a process, for example, the electrical current or the fluorescence power, or the instantaneous rate of the photochemical reaction, whereas the relevant signal is $S = \int S(t) \, dt = S(\omega = 0)$. The detected signal S may be, for example, the total charge produced by the photodetector, the total energy released through fluorescence, or the total yield of photochemical product. According to eq 7, the signal at order n reads

$$S^{(n)} = \int R^{(n)}(0, \omega_1 + \ldots + \omega_{n-1}, \ldots, \omega_1) E(\omega_n) \ldots$$

$$E(\omega_1) \frac{d\omega_1}{2\pi} \ldots \frac{d\omega_{n-1}}{2\pi} \quad (12)$$

with the convention $\omega_n = -\omega_1 - \ldots - \omega_{n-1}$. The final signal thus results from the nonlinear mixing between the frequency components of the field to eventually produce a DC contribution. If the pulse spectrum is centered at frequency ω_0, each interaction with the field will add $\pm\omega_0$. Unless the spectra are extremely broad (i.e., comparable to one octave), only an even number of interactions will produce a DC component. In the following, we consider the cases of second- and fourth-order processes.

3.1. One-Photon Detection. Let us consider here the case of a signal quadratic in the electric field or linear in the pulse energy, which can also be described as a one-photon process (two field interactions). We then have

$$S^{(2)}(t) =$$

$$\int R^{(2)}(\omega_1 + \omega_2, \omega_1) E(\omega_2) E(\omega_1) \exp(-i(\omega_1 + \omega_2)t) \frac{d\omega_1}{2\pi} \frac{d\omega_2}{2\pi} \quad (13)$$

and according to eq 12, the final signal reads

$$S^{(2)} = \int R^{(2)}(0, \omega_1) E(-\omega_1) E(\omega_1) \frac{d\omega_1}{2\pi} = \int g^{(1)}(\omega) |E(\omega)|^2 \frac{d\omega}{2\pi} \quad (14)$$

The quantity $g^{(1)}(\omega) = R^{(2)}(0, \omega)$ can be clearly related to the excitation spectrum of the process under consideration, which can be measured either by a narrowband light source whose wavelength is tuned or by a Fourier transform spectroscopy approach employing two pulse replicas whose temporal distance is scanned.[5] The final signal $S^{(2)}$ (e.g., the population transferred in a one-photon excitation probed after all coherent processes induced by the pump laser have faded) hence

is insensitive to the phase of the electric field.[6-8] This has also been pointed out recently[9] with regard to coherent control in the low-excitation regime.[10] In contrast, nonstationary signals can be coherently controlled even for signals quadratic in the electric field,[11] like vibrational wave packet evolution[7,12] or coherent transients,[8,13] but also here, the final (or time-integrated) result will be independent of the phase of the electric field.

3.2. Two-Photon Detection. We now have four field interactions, and eq 6 takes the form $S^{(4)}(t) = R^{(4)} \odot [EEEE]$, describing two-photon processes such as two-photon absorption or two-photon excited fluorescence but, for example, also the first nonlinear term in absorption saturation.

According to eq 12, two-photon absorption will be governed by a 3D response function $R^{(4)}(0, \omega_1 + \omega_2 + \omega_3, \omega_1 + \omega_2, \omega_1)$, which is particularly rich when there is an intermediate resonant level, giving rise to remarkable effects in coherent control scenarios.[14,15] A 2D projection of this 3D response function has also been measured by use of multidimensional spectroscopy associated with phase cycling.[16]

In the absence of an intermediate level, the pulse must induce a coherence oscillating at $\pm 2\omega_0$ after two field interactions so that, when $E = (\mathcal{E} + \mathcal{E}^*)/2$ is expanded, only 2 out of the 16 possible terms are relevant:

$$S^{(4)}(t) = \frac{1}{16} R^{(4)} \odot ([\mathcal{E}^* \mathcal{E}^* \mathcal{E} \mathcal{E}] + [\mathcal{E} \mathcal{E} \mathcal{E}^* \mathcal{E}^*]) \qquad (15)$$

Indeed, without relying too much on a particular microscopic model, we can state that after the first and third interaction, the system must be in a short-lived coherence due to the lack of an intermediate level. This implies that in the frequency domain, $R^{(4)}$ varies slowly with respect to its second and last arguments, which can be replaced with the pulse center frequency. Equation 12 thus reduces to

$$S^{(4)} = \frac{1}{8} \mathcal{R} \left\{ \int R^{(4)}(0, \omega_0, \omega, \omega_0) \mathcal{E}(\omega - \omega_3)^* \mathcal{E}(\omega_3)^* \times \right.$$
$$\left. \mathcal{E}(\omega - \omega_1) \mathcal{E}(\omega_1) \frac{d\omega_1}{2\pi} \frac{d\omega_3}{2\pi} \frac{d\omega}{2\pi} \right\} \qquad (16)$$

where $\mathcal{R}$ stands for the real part. This integral involves two convolution products of the form $\mathcal{E}^{(2)}(\omega) = \mathcal{E}(\omega) \otimes \mathcal{E}(\omega)$ where $\mathcal{E}^{(2)}$ is by definition the two-photon field. In time domain, the two-photon field is simply the square of the incident field, that is, $\mathcal{E}^{(2)}(t) = \mathcal{E}(t)^2$. Introducing $g^{(2)}(\omega) = (1/8) \mathcal{R}\{R^{(4)}(0, \omega_0, \omega, \omega_0)\}$ allows eq 16 to be reduced to

$$S^{(4)} = \int g^{(2)}(\omega) |\mathcal{E}^{(2)}(\omega)|^2 \frac{d\omega}{2\pi} \qquad (17)$$

Note the analogy to eq 14, with the difference that the signal is now entirely driven by the two-photon field, as previously reported.[17-19] The final yield is simply the overlap integral between the spectrum of the two-photon field and the appropriate two-photon spectrum $g^{(2)}(\omega)$, which, depending on the actual experiment, can be the two-photon absorption spectrum or the excitation spectrum of the two-photon excited fluorescence, for example. As in the case of one-photon absorption, the two-photon spectrum can be measured either using a tunable narrow-band laser[20] or by Fourier transform spectroscopy.[21] Phase shaping of the incident field results in an amplitude shaping of the two-photon spectrum, allowing coherent control of two-photon absorption.[22]

4. Multidimensional Spectroscopy

For nonlinear signals, a one-dimensional visualization conceals important information, which can be accessed by a multidimensional representation. This is in analogy to nuclear magnetic resonance spectroscopy (NMR),[23] where multidimensional methods have replaced conventional one-dimensional ones, but brought forward to the optical spectral regime and ultrafast time scales. Many outstanding experimental and theoretical achievements have been reported recently,[4,24,25] as also highlighted in this special issue. The most comprehensive description is the nonlinear response function, and hence the ultimate goal for experiments is its complete determination.

4.1. Second-Order Response. The electric field radiated at the second order of perturbation theory reads

$$E^{(2)}(t) = \Xi^{(2)} \otimes [EE] \qquad (18)$$

According to eq 5, the region where $\Xi^{(2)}(\omega_2, \omega_1)$ is addressed corresponds to the areas where the 2D function $E(\omega_2)E(\omega_1)$ is nonzero. Using eq 2, we obtain four such regions, as shown in Figure 1a. The term in $\mathcal{E}(\omega_2)\mathcal{E}(\omega_1)$ corresponds to a case where both ω_1 and ω_2 are positive, which results in a generated frequency $\omega_1 + \omega_2$ close to $2\omega_0$ (sum-frequency mixing or second-harmonic generation). In contrast, the term in $\mathcal{E}(\omega_2)\mathcal{E}^*(-\omega_1)$ correponds to a situation where ω_1 is negative, so the generated frequency $\omega_1 + \omega_2 = |\omega_2| - |\omega_1|$ is close to zero frequency (difference-frequency mixing or optical rectification).

As in 2D NMR, the measurement of the second-order response function $\Xi^{(2)}(\omega_2, \omega_1)$ by 2D spectroscopy[3,26] relies on exciting the system with a sequence of two pulses, $E(t) + E(t + \tau)$ or $E(\omega)(1 + \exp(-i\omega\tau))$ in frequency domain. The field resulting from the interaction between these two pulses is measured as a function of the time delay τ in both amplitude and phase, using, for example, frequency-[26] or time-domain interferometry.[3] The contribution to the radi-

ated field resulting from the mixing between the two pulses reads

$$E(\omega, \tau) = 2 \int \Xi^{(2)}(\omega - \omega_1, \omega_1) E(\omega - \omega_1) E(\omega_1) \times$$

$$\exp(-i\omega_1\tau) \frac{d\omega_1}{2\pi} \quad (19)$$

An inverse Fourier transform of this quantity with respect to τ directly yields

$$E(\omega, \omega_\tau) = 2\Xi^{(2)}(\omega - \omega_\tau, \omega_\tau) E(\omega - \omega_\tau) E(\omega_\tau) \quad (20)$$

A complete knowledge, in both amplitude and phase, of the exciting field allows the division of $E(\omega,\omega_\tau)$ by the complex quantity $E(\omega - \omega_\tau)E(\omega_\tau)$, yielding the response function $\Xi^{(2)}(\omega - \omega_\tau,\omega_\tau)$. Note that this procedure allows the retrieval of the response function in the areas spanned by the exciting field (shown in Figure 1) and that it is exact even in the case of pulses of finite duration. This approach has been demonstrated in the cases of sum-frequency mixing[26] and difference-frequency mixing[3] in situations where the second-order response function was deliberately dominated by phase-matching effects. It would be of great interest to broaden the frequency range covered by such a method in order to address large areas of the second-order susceptibility. Figure 1 illustrates both the symmetrized, as calculated from the sum-over-state expression of $\chi^{(2)}(\omega_2,\omega_1)$,[1] and the time-ordered response function that could be obtained in the case of a three-level system.

4.2. Third-Order Response. At the third order of perturbation theory, we have

$$E^{(3)}(t) = \Xi^{(3)} \otimes [EEE] \quad (21)$$

Similar to the second-order response, the region where $\Xi^{(3)}(\omega_3,\omega_2,\omega_1)$ is addressed corresponds to the areas where the 3D function $E(\omega_3)E(\omega_2)E(\omega_1)$ is nonzero. Since each field is associated with a frequency $\pm\omega_0$, depending on which complex component contributes to the interaction, the addressed area of the response function corresponds to eight spheres whose diameters correspond to the pulse spectral width and which are centered at the eight vertices of a cube. However, in its conventional implementation,[27] multidimensional spectroscopy of the third-order response is better understood by use of the time-ordered response function $R^{(3)}$ rather than the symmetrized response Ξ, that is, $E^{(3)}(t) = R^{(3)} \odot [EEE]$. Taking the Fourier transform of eq 7, we can write the field radiated at frequency ω

$$E^{(3)}(\omega) = \int R^{(3)}(\omega, \omega_T, \omega_\tau) E(\omega - \omega_T) E(\omega_T - \omega_\tau) E(\omega_\tau) \frac{d\omega_T}{2\pi} \frac{d\omega_\tau}{2\pi} \quad (22)$$

where we have made the change of variable $\omega_\tau = \omega_1$, $\omega_T = \omega_1 + \omega_2$, and $\omega = \omega_1 + \omega_2 + \omega_3$. The values of ω, ω_T, and ω_τ that can be addressed can then be determined by keeping track of the possible excitation paths, as shown in Figure 2a. As above, there are eight regions that can be addressed by the exciting field. If the spectral width is smaller than one octave, these areas do not overlap and it is possible to define specific parts of the response function corresponding to a response $R_{\varepsilon_3,\varepsilon_2,\varepsilon_1}$ where $\varepsilon_k = \pm 1$ corresponds to the sign of the complex component contributing to the kth interaction. Figure 2b shows three slices of the 3D response function $R(\omega, \omega_T, \omega_\tau)$ for three different values of ω_T.
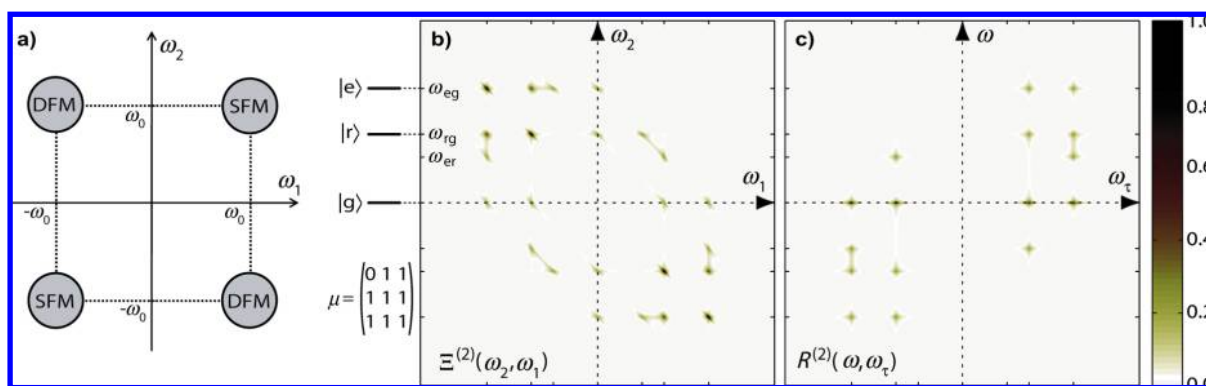

FIGURE 1. (a) Areas of the response function $\Xi^{(2)}(\omega_2,\omega_1)$ addressed by a short pulse of center frequency ω_0. Regions where ω_1 and ω_2 have the same sign correspond to sum-frequency mixing (SFM) and those with different signs to difference-frequency mixing (DFM). (b) Example of a second-order symmetrized response function $\Xi^{(2)}(\omega_2,\omega_1)$ for a three-level system with the indicated dipole matrix, exhibiting both single resonances (lines associated with ω_1, ω_2, or $\omega_1 + \omega_2$ resonant with a transition) and double resonances (peaks at intersections of single resonance lines). (c) The corresponding time-ordered response function $R^{(2)}(\omega,\omega_\tau)$. While $\Xi^{(2)}(\omega_2,\omega_1)$ generally shows all possible combinations for two frequencies, ω_1 and ω_2, each interacting with the system once, $R^{(2)}(\omega,\omega_\tau)$ reveals the polarization's frequency ω_τ after the first and ω after the second interaction, respectively. Absolute values are plotted for a Bloch equation model with $T_1 = 2.5T_2$.
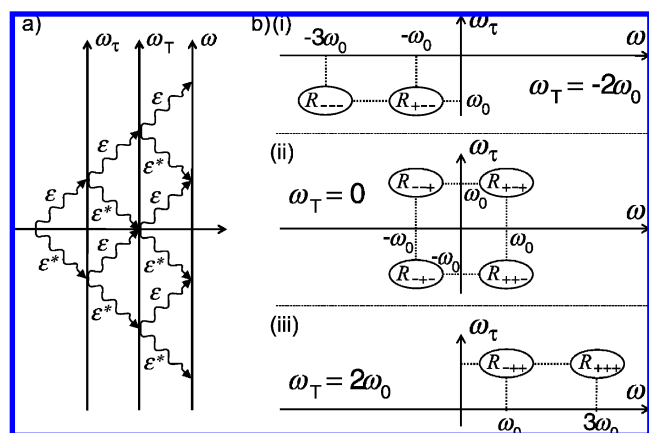
FIGURE 2. (a) Possible paths of excitation of the response function $R(\omega, \omega_T, \omega_\tau)$. Each interaction either adds ($\mathscr{E}$) or subtracts ($\mathscr{E}^*$) a frequency close to the center frequency ω_0. (b) Representation of three 2D slices of addressed areas of the response function $R(\omega, \omega_T, \omega_\tau)$ for $\omega_T = -2\omega_0$ (i), $\omega_T = 0$ (ii), and $\omega_T = 2\omega_0$ (iii).

Four terms are complex conjugates of the other four, so in the following we will consider only terms contributing to $\mathscr{E}^{(3)}(t)$, which means that the final frequency ω must be positive. One of the four terms, R_{+++}, corresponds to third-harmonic generation, which will not be discussed here. The three remaining terms are the two-quantum term R_{-++} [$\omega_T = 2\omega_0$, Figure 2b(iii)], and the one-quantum terms R_{++-} and R_{+-+} exhibiting $\omega_T = 0$ [Figure 2b(ii)] and corresponding, respectively, to rephasing (ω and ω_τ have opposite sign) and non-rephasing (same sign) contributions.

Let us consider the boxcar geometry with E_1, E_2 and E_3, that is, a geometrical arrangement of laser beams selecting the signal detected in direction $\mathbf{k}_4 = -\mathbf{k}_1 + \mathbf{k}_2 + \mathbf{k}_3$. The field radiated in this direction reads

$$\mathscr{E}^{(3)}(t) = \frac{6}{4} \xi^{(3)} \odot [\mathscr{E}_3 \mathscr{E}_2 \mathscr{E}_1^*] \quad (23)$$

Note that we use here the function $\xi^{(3)}$ rather than $R^{(3)}$ so that the different ordering of the three fields contribute equally to the response; hence the factor of $6 = 3!$. Therefore, it is not necessary to explicitly write down the six possible permutations of the interactions as would be otherwise required. We call τ the time delay between pulses 1 and 2 and T the time delay between pulses 2 and 3, which are assumed to arrive in this order for positive values of the time delays. In frequency domain, we thus have $\mathscr{E}_3(\omega) = \mathscr{E}(\omega)$, $\mathscr{E}_2(\omega) = \mathscr{E}(\omega) \exp(-i\omega T)$, and $\mathscr{E}_1(\omega) = \mathscr{E}(\omega) \exp(-i\omega(\tau + T))$. We then obtain

$$\mathscr{E}^{(3)}(\omega, T, \tau) = \frac{6}{4} \int \xi^{(3)}(\omega, \omega_T, \omega_\tau) \mathscr{E}(\omega - \omega_T) \mathscr{E}(\omega_T - \omega_\tau) \times$$
$$\mathscr{E}^*(-\omega_\tau) \, e^{-i\omega_T T - i\omega_\tau \tau} \frac{d\omega_T}{2\pi} \frac{d\omega_\tau}{2\pi} \quad (24)$$

If we assume this quantity to be measured as a function of T and τ, scanned for both negative and positive values, a 2D inverse Fourier transform with respect to T and τ yields

$$\mathscr{E}^{(3)}(\omega, \omega_T, \omega_\tau) = \frac{3}{2} \xi^{(3)}(\omega, \omega_T, \omega_\tau) \mathscr{E}(\omega - \omega_T) \mathscr{E}(\omega_T - \omega_\tau) \times$$
$$\mathscr{E}^*(-\omega_\tau) \quad (25)$$

Such an experiment will yield all the information on the third-order response through the entire 3D response function $\xi^{(3)}(\omega, \omega_T, \omega_\tau)$, that is, full third-order 3D spectroscopy. Such an approach necessitates a Fourier transform with respect to T, like very recently performed[28] but only of $|\mathscr{E}(\omega, T, \omega_\tau)|$. The advantage of full third-order 3D spectroscopy is that, as for the second-order response, the spectral amplitude and phase of the exciting pulse can be taken into account so that the method is exact even for pulses of finite duration (and even with chirp if the pulse is fully characterized). Finally, it should be noted that we get $\xi^{(3)}$ rather than $R^{(3)}$, which can however be obtained from $\xi^{(3)}$ as shown in the first section. As an example, Figure 3 juxtaposes and discusses $R^{(3)}$ and $\Xi^{(3)}$ of a three-level system for two different coupling schemes.

In practice, multidimensional spectroscopy is usually implemented in 2D rather than 3D, that is, measuring 2D projections of the full 3D response function. As a consequence, we will have to make approximations, namely, that the pulses are sufficiently short so that there is no need to care about what happens when the pulses overlap. In the following, we will consider only the case where the waiting time T is positive (i.e., greater than the pulse duration). Let us first consider the case where the time delay τ is positive. With the assumption that the pulses are short enough, the time ordering of the three interactions is clearly $\mathscr{E}_1$, then $\mathscr{E}_2$, and finally $\mathscr{E}_3$. The only contribution to the detected field is therefore

$$\mathscr{E}^{(3)}(t, T, \tau) = \frac{1}{4} R^{(3)} \odot [\mathscr{E}_3 \mathscr{E}_2 \mathscr{E}_1^*] \quad (26)$$

Only R_{++-} will contribute to the signal in the boxcar geometry, so this pulse ordering selects the rephasing term of the response function.[27] We therefore obtain an expression very similar to eq 24, except that $\xi(\omega, \omega_T, \omega_\tau)$ can be replaced with $R_{++-}(\omega, \omega_T, \omega_\tau)/6$. Using the approximation of infinitely short pulses, we can also replace in the integral the frequency-dependent fields by a constant value E_0, so eq 24 becomes a 2D Fourier transform of $R_{++-}(\omega, \omega_T, \omega_\tau)$.

By performing an inverse Fourier transform with respect to ω_τ, we thus obtain

$$\mathcal{E}_R^{(3)}(\omega, T, \omega_\tau) = \frac{E_0^3}{4} R_{++-}(\omega, T, \omega_\tau) \qquad (27)$$

which is the usual rephasing 2D spectrum $R_{++-}(\omega, T, \omega_\tau)$. Similarly, the data recorded by permuting pulses 1 and 2 yields the non-rephasing 2D spectrum

$$\mathcal{E}_{NR}^{(3)}(\omega, T, \omega_\tau) = \frac{E_0^3}{4} R_{+-+}(\omega, T, \omega_\tau) \qquad (28)$$

4.3. Multidimensional Spectroscopy in Pump−Probe Geometry.

Let us now consider the use of the pump−probe geometry for multidimensional spectroscopy. This can be either achieved with a spectrally narrow pump (performing the first two interactions) whose center frequency is tuned across the spectrum,[29] or again by Fourier transform multidimensional spectroscopy in which the pump field comprises two pulses.[27]

The experiment consists of recording the pump-induced change in transmitted probe intensity, $\Delta I(\omega) = 2\mathcal{R}\{\mathcal{E}'^{*}(\omega)\mathcal{E}^{(3)}(\omega)\}$, which results from the interference between the transmitted probe (in the absence of the pump), $\mathcal{E}'(\omega)$, and the radiated third-order field

$$\mathcal{E}^{(3)}(t) = \frac{6}{4} \xi^{(3)} \odot [\mathcal{E}_T \mathcal{E}_P \mathcal{E}_P^{*}] \qquad (29)$$

which involves two interactions with the pump field $\mathcal{E}_P$, and one with the probe $\mathcal{E}_T$. In the case of an optically thin sample, it can be assumed that the transmitted probe $\mathcal{E}'(\omega)$ is identical to the incident probe field. For an infinitely short probe pulse, the measured signal is then simply proportional
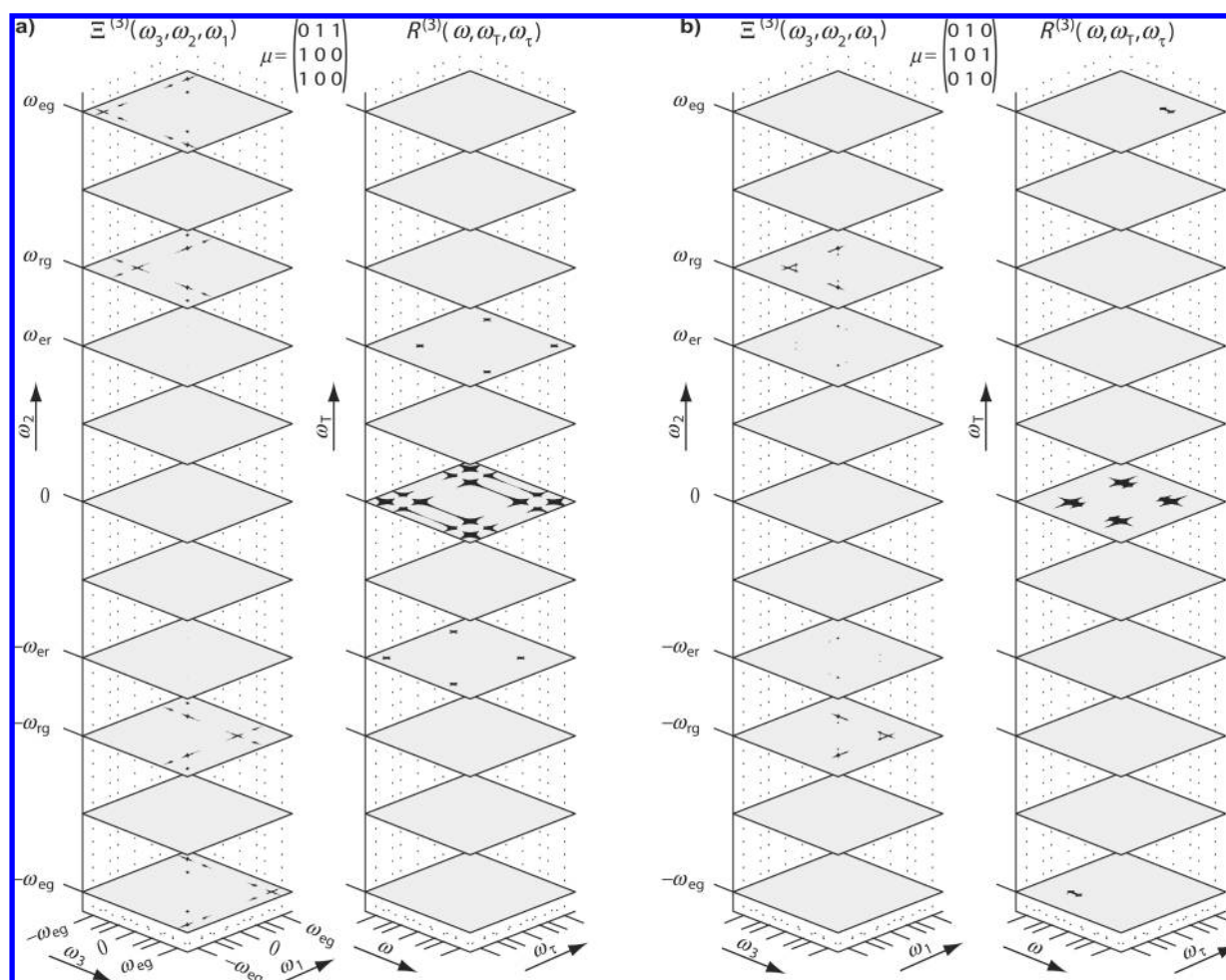

FIGURE 3. Slices through the absolute value of 3D response functions for the three-level system of Figure 1 for two different dipole matrices μ. (a) States $|r\rangle$ and $|e\rangle$ share a common ground state $|g\rangle$ but are not directly coupled. $\Xi^{(3)}(\omega_3, \omega_2, \omega_1)$ reveals all combinations of the three interacting frequencies, while $R^{(3)}(\omega, \omega_T, \omega_\tau)$, for example, directly reveals possible quantum beats (at $\omega_T = \pm\omega_{er}$) after the second interaction. (b) The states form a ladder where $|g\rangle$ and $|e\rangle$ are not directly coupled. Thus, $\Xi^{(3)}$ has no contribution at $\omega_n = \pm\omega_{eg}$. By contrast, in $R^{(3)}$ the two-quantum states show up at $\omega_T = \pm\omega_{eg}$; For clarity, contributions larger than 4% of the maximum are set to black.

Ⓦ Movies in AVI format of the left and right parts of panel a and of the left and right parts of panel b are available.

to the real part of the third-order field. Alternatively, the transmitted probe can be fully characterized so that the experimental data can be numerically processed in order to produce the real part of the third-order field. In either case, we will assume in the following that we have access to the quantity

$$S(\omega) = \mathscr{E}^{(3)}(\omega) + \mathscr{E}^{(3)}(\omega)^* \quad (30)$$

Note that for a positive waiting time, the probe field can be assumed to be the last one interacting with the system, so that the use of the time-ordered response function yields

$$\mathscr{E}^{(3)}(t) = \frac{1}{4}(R_{++-}^{(3)} \odot [\mathscr{E}_T \mathscr{E}_p \mathscr{E}_p^*] + R_{+-+}^{(3)} \odot [\mathscr{E}_T \mathscr{E}_p^* \mathscr{E}_p]) \quad (31)$$

We will briefly focus on the Fourier transform implementation of multidimensional spectroscopy in the pump–probe geometry,[27] as has been recently demonstrated experimentally.[30–33] The method comprises the same scanning protocol as the boxcars implementation, except that pulses $\mathscr{E}_1$ and $\mathscr{E}_2$ are collinear and constitute the pump pulse. Equation 30 will then both comprise pure pump–probe contributions (varying very slowly with respect to τ, as the first two interactions come from the same pulse of the pump field) that can be removed, for example, by Fourier filtering, and the desired echo signals, which will be considered in the following. Both rephasing and non-rephasing terms will contribute to $\mathscr{E}^{(3)}(\omega, T, \tau)$ simultaneously. Scanning only positive values of τ, we obtain

$$\mathscr{E}^{(3)}(\omega, T, \omega_\tau) = \frac{E_0^{\,3}}{4}(R_{++-}(\omega, T, \omega_\tau) + R_{+-+}(\omega, T, \omega_\tau)) \quad (32)$$

where the two terms can be easily separated since they correspond to different signs of the frequency ω_τ. However, the measured quantity is actually $S(\omega, T, \tau)$, as given by eq 30. The Fourier transform with respect to τ of the real part of the third-order field results in a symmetrization in ω_τ space, producing an overlap between the rephasing and non-rephasing term both at positive and at negative values of ω_τ, and yielding only the absorptive 2D spectrum

$$R_{abs}^{(3)}(\omega, T, \omega_\tau) = \mathscr{R}\{R_{++-}^{(3)}(\omega, T, -\omega_\tau) + R_{+-+}^{(3)}(\omega, T, \omega_\tau)\} \quad (33)$$

Nonetheless, it is still possible to retrieve independently the rephasing and non-rephasing terms by making use of causality (i.e., doing an inverse Fourier transform back to t space and only keeping contributions for $t > 0$) for extracting the complex field from its real part, as most recently demonstrated experimentally.[33] This implementation of 2D spectroscopy thus provides information which is as useful as that provided by the boxcar geometry, with the advantage that no additional phasing measurement[27,34,35] is needed to determine the absolute phase of the spectra.

5. Higher-Order Response

We also want to briefly mention processes of even higher order and their implications in nonlinear spectroscopy. More interactions of the electric field and the material are described by higher-order response functions. The increased number of degrees of freedom may lead to a broader versatility in coherent control, for example, in three-photon absorption[19] described by a response function $\Xi^{(6)}(\omega_6, ..., \omega_1)$, where the system interacts six times with the electric field whose spectral phase, amplitude, and polarization can be manipulated independently.

In multidimensional spectroscopy, the higher nonlinearity allows the revelation of information not accessible in a similar way otherwise, for instance, in fifth order described by $\Xi^{(5)}(\omega_5, ..., \omega_1)$. Two-dimensional fifth-order Raman spectroscopy, with two nonresonant pump pulse pairs separated in time and followed by a probe pulse, is a very sensitive method for measuring the many-body potential of liquids.[36] In a different approach called fifth-order 3D spectroscopy[37,38] (not to be confused with third-order 3D spectroscopy mentioned earlier) the five pulses are all resonant and are moved independently in time, augmenting the benefits of third-order 2D spectroscopy, for example, by covering higher-lying levels, rephasing two-quantum coherences, and being sensitive to non-Gaussian frequency fluctuations.

Finally, we stress that in the case of strong-field interactions perturbation theory breaks down and effects beyond the approach of a multidimensional response become dominant.

6. Conclusion

We have discussed a global multidimensional response function analogous to the microscopic nonlinear susceptibility. Its advantage of being a very general quantity not limited to certain properties of the interacting electric field or the system under study has been discussed in the context of coherent control and multidimensional spectroscopy. Thus, a global response function is helpful for the elucidation of nonlinear optical processes and possibly also for the conception of novel techniques to measure them.

BIOGRAPHICAL INFORMATION

Patrick Nuernberger (Ph.D., Physics, 2007, Universität Würzburg) is a Leopoldina postdoctoral fellow at Ecole Polytechnique, investigating the dynamics of biological systems using different ultrafast spectroscopic methods and coherent control approaches.

Kevin F. Lee (Ph.D., Physics, 2006, McMaster University) is a postdoctoral researcher and instructor at Ecole Polytechnique, studying proteins using multidimensional spectroscopy. He previously performed research on molecular alignment control at the National Research Council Canada.

Manuel Joffre (Ph.D., Physics, 1989, Université Paris VI) is a Directeur de Recherche at CNRS and Associate Professor at Ecole Polytechnique who is leading research projects on multidimensional spectroscopy in proteins and coherent control for nonlinear microscopy in biological organisms.

REFERENCES

1 Butcher, P. N.; Cotter, D. *The Elements of Nonlinear Optics*; Cambridge University Press: Cambridge, U.K., 1990.

2 Mukamel, S. *Principles of Nonlinear Optical Spectroscopy*; Oxford University Press: New York, 1995.

3 Belabas, N.; Joffre, M. Visible-infrared two-dimensional Fourier-transform spectroscopy. *Opt. Lett.* **2002**, *27*, 2043–2045.

4 Jonas, D. M. Two-Dimensional Femtosecond Spectroscopy. *Annu. Rev. Phys. Chem.* **2003**, *54*, 425–463.

5 Griffiths, P. R.; de Haseth, J. A. *Fourier Transform Infrared Spectrometry*; Wiley: New York, 1986.

6 Brumer, P.; Shapiro, M. One photon mode selective control of reactions by rapid or shaped laser pulses: An emperor without clothes? *Chem. Phys.* **1989**, *139*, 221–228.

7 Bardeen, C. J.; Wang, Q.; Shank, C. V. Femtosecond chirped pulse excitation of vibrational wave packets in LD690 and bacteriorhodopsin. *J. Phys. Chem. A* **1998**, *102*, 2759–2766.

8 Dudovich, N.; Oron, D.; Silberberg, Y. Coherent transient enhancement of optically induced resonant transitions. *Phys. Rev. Lett.* **2002**, *88*, 123004.

9 Joffre, M. Comment on "Coherent control of retinal isomerization in bacteriorhodopsin". *Science* **2007**, *317*, 453.

10 Prokhorenko, V. I.; Nagy, A. M.; Waschuk, S. A.; Brown, L. S.; Birge, R. R.; Miller, R. J. D. Coherent control of retinal isomerization in bacteriorhodopsin. *Science* **2006**, *313*, 1257–1261.

11 Krause, J. L.; Whitnell, R. M.; Wilson, K. R.; Yan, Y. J.; Mukamel, S. Optical control of molecular-dynamics - molecular cannons, reflectrons, and wave-packet focusers. *J. Chem. Phys.* **1993**, *99*, 6562–6578.

12 Yan, Y. J.; Gillilan, R. E.; Whitnell, R. M.; Wilson, K. R.; Mukamel, S. Optical control of molecular-dynamics: Liouville-space theory. *J. Phys. Chem.* **1993**, *97*, 2320–2333.

13 Zamith, S.; Degert, J.; Stock, S.; de Beauvoir, B.; Blanchet, V.; Bouchene, M. A.; Girard, B. Observation of coherent transients in ultrashort chirped excitation of an undamped two-level system. *Phys. Rev. Lett.* **2001**, *87*, 033001.

14 Dudovich, N.; Dayan, B.; Gallagher Faeder, S. M.; Silberberg, Y. Transform-limited pulses are not optimal for resonant multiphoton transitions. *Phys. Rev. Lett.* **2001**, *86*, 47–50.

15 Chatel, B.; Degert, J.; Stock, S.; Girard, B. Competition between sequential and direct paths in a two-photon transition. *Phys. Rev. A* **2003**, *68*, 041402.

16 Tian, P.; Keusters, D.; Suzaki, Y.; Warren, W. S. Femtosecond phase-coherent two-dimensional spectroscopy. *Science* **2003**, *300*, 1553–1555.

17 Salour, M. M. Quantum interference effects in 2-photon spectroscopy. *Rev. Mod. Phys.* **1978**, *50*, 667–681.

18 Broers, B.; Noordam, L. D.; Vandenheuvell, H. B. V. Diffraction and focusing of spectral energy in multiphoton processes. *Phys. Rev. A* **1992**, *46*, 2749–2756.

19 Walowicz, K. A.; Pastirk, I.; Lozovoy, V. V.; Dantus, M. Multiphoton intrapulse interference. 1. Control of multiphoton processes in condensed phases. *J. Phys. Chem. A* **2002**, *106*, 9369–9373.

20 Xu, C.; Webb, W. W. Measurement of two-photon excitation cross sections of molecular fluorophores with data from 690 to 1050 nm. *J. Opt. Soc. Am. B* **1996**, *13*, 481–491.

21 Ogilvie, J. P.; Kubarych, K. J.; Alexandrou, A.; Joffre, M. Fourier transform measurement of two-photon excitation spectra: Applications to microscopy and optimal control. *Opt. Lett.* **2005**, *30*, 911–913.

22 Meshulach, D.; Silberberg, Y. Coherent quantum control of two-photon transitions by a femtosecond laser pulse. *Nature* **1998**, *396*, 239–242.

23 Ernst, R.; Bodenhausen, G.; Wokaun, A. *Principles of Nuclear Magnetic Resonance in One and Two Dimensions*; Clarendon Press: Oxford, U.K., 1997.

24 Hochstrasser, R. Multidimensional ultrafast spectroscopy special feature. *Proc. Natl. Acad. Sci. U.S.A.* **2007**, *104*, 14189–14242.

25 Cho, M. Coherent two-dimensional optical spectroscopy. *Chem. Rev.* **2008**, *108*, 1331–1418.

26 Lepetit, L.; Joffre, M. Two-dimensional nonlinear optics using Fourier-transform spectral interferometry. *Opt. Lett.* **1996**, *21*, 564–566.

27 Gallagher Faeder, S. M.; Jonas, D. M. Two-dimensional electronic correlation and relaxation spectra: Theory and model calculations. *J. Phys. Chem. A* **1999**, *103*, 10489–10505.

28 Nee, M. J.; Baiz, C. R.; Anna, J. M.; McCanne, R.; Kubarych, K. J. Multilevel vibrational coherence transfer and wavepacket dynamics probed with multidimensional IR spectroscopy. *J. Chem. Phys.* **2008**, *129*, 084503.

29 Cervetto, V.; Helbing, J.; Bredenbeck, J.; Hamm, P. Double-resonance versus pulsed Fourier transform two-dimensional infrared spectroscopy: An experimental and theoretical comparison. *J. Chem. Phys.* **2004**, *121*, 5935–5942.

30 Shim, S. H.; Strasfeld, D. B.; Ling, Y. L.; Zanni, M. T. Automated 2D IR spectroscopy using a mid-IR pulse shaper and application of this technology to the human islet amyloid polypeptide. *Proc. Natl. Acad. Sci. U.S.A.* **2007**, *104*, 14197–14202.

31 Grumstrup, E. M.; Shim, S. H.; Montgomery, M. A.; Damrauer, N. H.; Zanni, M. T. Facile collections of two-dimensional electronic spectra using femtosecond pulse-shaping technology. *Opt. Express* **2007**, *15*, 16681–16689.

32 DeFlores, L. P.; Nicodemus, R. A.; Tokmakoff, A. Two dimensonal Fourier transform spectroscopy in the pump-probe geometry. *Opt. Lett.* **2007**, *32*, 2966–2968.

33 Myers, J. A.; Lewis, K. L. M.; Tekavec, P. F.; Ogilvie, J. P. Two-color two-dimensional Fourier transform electronic spectroscopy with a pulse-shaper. *Opt. Express* **2008**, *16*, 17420–17428.

34 Brixner, T.; Mančal, T.; Stiopkin, I. V.; Fleming, G. R. Phase-stabilized two-dimensional electronic spectroscopy. *J. Chem. Phys.* **2004**, *121*, 4221–4236.

35 Park, S.; Kwak, K.; Fayer, M. D. Ultrafast 2D-IR vibrational echo spectroscopy: A probe of molecular dynamics. *Laser Phys. Lett.* **2007**, *4*, 704–718.

36 Kubarych, K.; Milne, C.; Miller, R. J. D. Fifth-order two-dimensional Raman spectroscopy: A new direct probe of the liquid state. *Int. Rev. Phys. Chem.* **2003**, *22*, 497–532.

37 Hamm, P. Three-dimensional-IR spectroscopy: Beyond the two-point frequency fluctuation correlation function. *J. Chem. Phys.* **2006**, *124*, 124506.

38 Ding, F.; Zanni, M. T. Heterodyned 3D IR spectroscopy. *Chem. Phys.* **2007**, *341*, 95–105.